

Interface Engineering of Graphdiyne ($g\text{-C}_n\text{H}_{2n-2}$) coupling with NiCoP for Constructing a Barrier-Free Electron Channel in Photocatalytic Hydrogen Evolution

Qing Chen¹, Kai Wang^{1,*}, Zhiliang Jin^{1,2}

1. School of Chemistry and Chemical Engineering, Key Laboratory for Chemical Engineering and Technology, State Ethnic Affairs Commission, Ningxia Key Laboratory of Solar Chemical Conversion Technology, North Minzu University, Yinchuan 750021, P.R. China

2. School of Chemistry and Civil Engineering, Shaoguan University, Shaoguan 512005, P. R. China

Corresponding author: kaiwang@nun.edu.cn (K. Wang).

1. Characterization

Crystalline structures were examined by X-ray diffraction (XRD, Rigaku Ultima IV) with $\text{Cu K}\alpha$ radiation ($\lambda = 1.5406 \text{ \AA}$), scanning from 5° to 80° (2θ) at a rate of $10^\circ \text{ min}^{-1}$. Surface chemical composition and oxidation states were analyzed using X-ray photoelectron spectroscopy (XPS, Thermo Scientific ESCALAB Xi+). The morphology and microstructure were characterized by scanning electron microscopy (SEM, ZEISS EVO-10) and high-resolution transmission electron microscopy (HRTEM, JEOL JEM-2100F). Optical absorption properties were measured via UV-Vis diffuse reflectance spectroscopy (PerkinElmer Lambda 750S) with BaSO_4 as a reference. Charge recombination behavior was evaluated through time-resolved and steady-state photoluminescence spectra collected on a fluorescence spectrometer (Horiba FLUOROMAX-4). Additionally, electron paramagnetic resonance (EPR, Bruker MEX plus) operating at 100 kHz modulation frequency was employed to detect light-induced reactive oxygen species.

2. Photocatalytic H_2 evolution experiments

The photocatalytic hydrogen evolution performance was assessed using a 62 mL sealed reactor, where 10 mg of catalyst was dispersed in 30 mL of an aqueous solution containing 10 vol% TEOA. The system was purged with N_2 to ensure an anaerobic environment before being illuminated under a 5 W simulated solar lamp. Evolved gas was sampled at 1 h intervals and quantified by gas chromatography (Tianmei GC7900, equipped with a TCD detector and a 13X column). The hydrogen yield was determined using the external standard method. Apparent quantum efficiency

(AQE) measurements employed a 300 W xenon lamp with bandpass filters ($\lambda = 420, 450, 475, 500$ and 520) to obtain wavelength-dependent activity. The calculation formula of AQE is as follows:

$$\text{AQE} = \frac{2 \times \text{the number of evolved hydrogen molecules}}{\text{the number of incident photons}} \times 100\%$$

3. Electrochemical measurements

Electrochemical measurements were performed with a three-electrode setup connected to a VersatAT 4-400 workstation. A saturated calomel electrode (SCE) and a platinum foil were used as the reference and counter electrodes, respectively. The working electrode was prepared by coating a homogenized slurry onto an indium tin oxide (ITO) substrate ($1 \times 2 \text{ cm}^2$). The slurry was obtained by ultrasonically dispersing 5 mg of the photocatalyst in 25 μL of a 0.1 wt% Nafion/ethanol solution for 30 min, followed by infrared drying. All tests were carried out in a 0.2 M Na_2SO_4 electrolyte under visible-light irradiation provided by a 300 W Xe lamp equipped with a 420 nm cutoff filter. Transient photocurrent was measured at a constant bias of -0.2 V vs. SCE. Mott-Schottky analysis was conducted from -1.0 to $+1.0 \text{ V}$ (vs. SCE) at a frequency of 1 kHz. Electrochemical impedance spectroscopy (EIS) was performed with a 10 mV AC amplitude over a frequency range of $0.1\text{--}10^4$ Hz. Linear sweep voltammetry (LSV) was executed at a scan rate of $0.01 \text{ V}\cdot\text{s}^{-1}$.

4. DFT calculation

First-principles calculations were carried out with the CASPTE module. The Perdew-Burke-Ernzerhof (PBE) generalized gradient approximation was adopted to describe exchange–correlation interactions, and a plane-wave basis set with a cutoff energy of 450 eV was used for geometry optimization and spin polarization was included. A vacuum layer of 15 Å was added normal to the surface to avoid spurious interactions from periodic boundaries when calculating the work function.

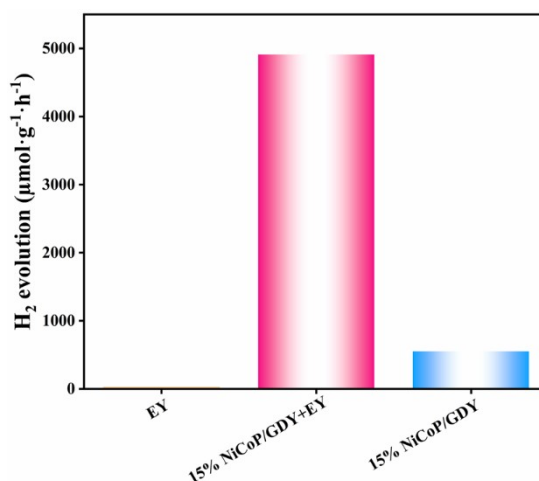


Fig. S1 The effect of eosin EY on the hydrogen evolution rate of the catalyst.

Table S1 TRPL decay parameters for GDY and 15% NiCoP/GDY

Samples	τ_1 [ns]	τ_2 [ns]	τ_{ave} [ns]
GDY	0.53 (96.25 %)	2.62 (3.75 %)	0.55
15% NiCoP/GDY	0.74 (94.54%)	2.56 (5.46 %)	0.78

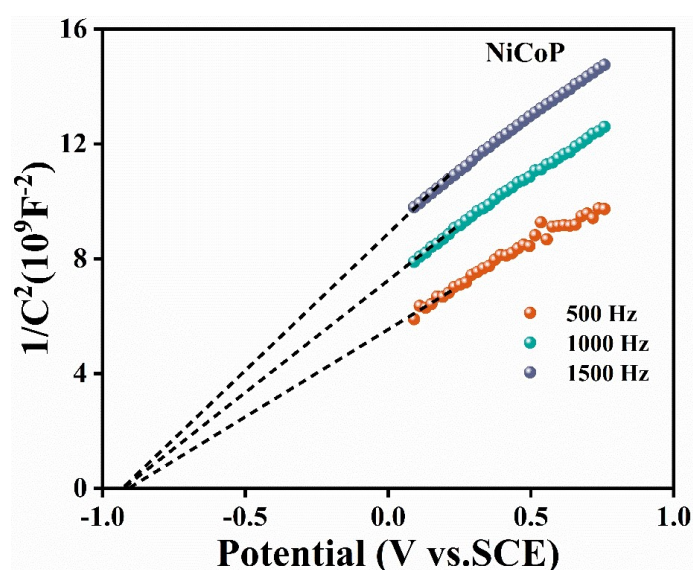


Fig. S2 Mott-Schottky plots of NiCoP.

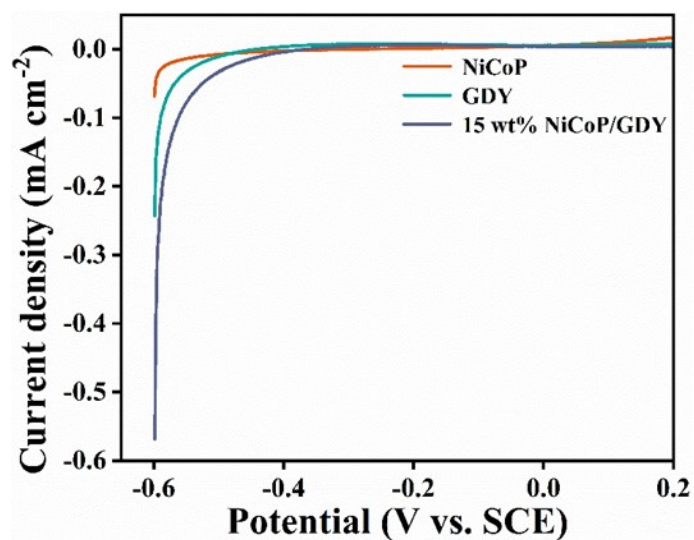


Fig. S3 LSV polarization curves of NiCoP, GDY and 15% NiCoP/GDY.

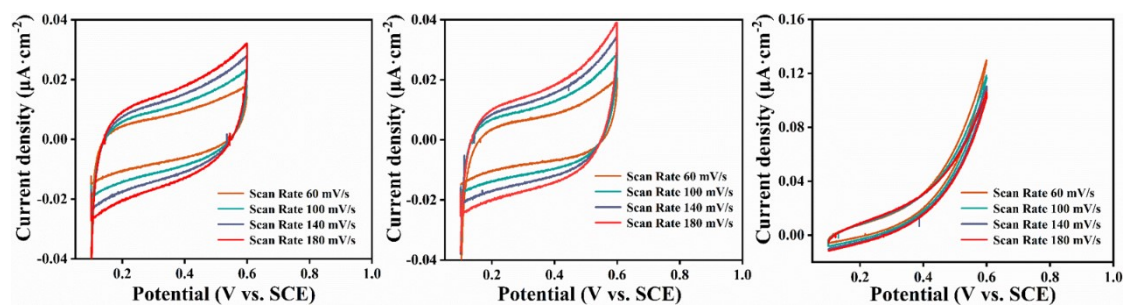


Fig. S4 CV curves at various scanning speeds for NiCoP, GDY and 15% NiCoP/GDY.

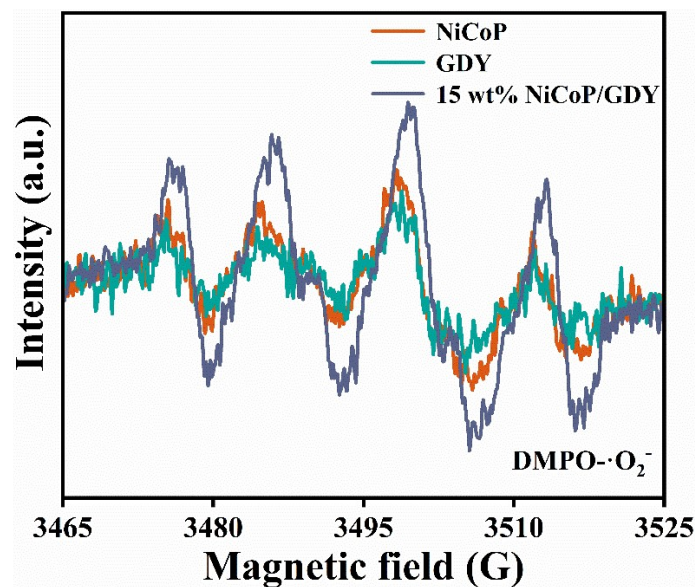


Fig. S5 DMPO·O₂⁻ signals under light irradiation of GDY, NiCoP and 15% NiCoP/GDY.

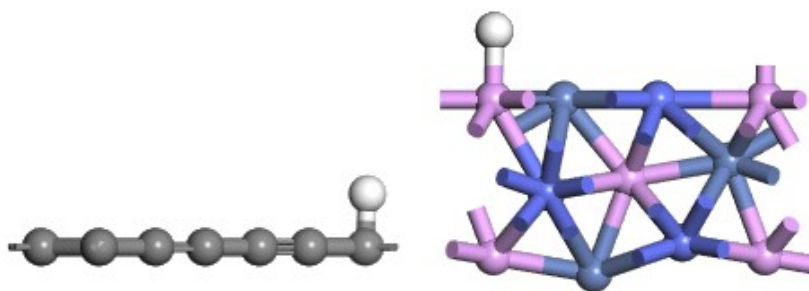


Fig. S6 The optimized hydrogen adsorption model of GDY and NiCoP.